

Apparent strangeness enhancement from multiplicity selection in high energy proton-proton collisions

Constantin Loizides

ORNL, Oak Ridge, TN, 37830, USA

Andreas Morsch

CERN, 1211 Geneva 23, Switzerland

September 14, 2021

Abstract

The increase of strange-particle yields relative to pions as a function of the event charged-particle multiplicity in proton-proton (pp) collisions at the LHC is argued to indicate the relevance of the final system produced in the collision. The rise with multiplicity (referred to as strangeness enhancement) is usually described by microscopic or hydrodynamical models as a result of the increasing density of produced partons or strings and their interactions. Instead, in this paper, we consider the multiple partonic interaction (MPI) picture originally developed in the context of the PYTHIA event generator to describe the rich structure of the underlying event in pp collisions. We find that strangeness enhancement in PYTHIA is hidden by a large excess of low- p_T multi-strange baryons, which mainly results from the hadronization of u -quark, d -quark and gluon (udg) strings. Strange baryons produced in strings formed from parton showers initiated by strange quarks (s -fragmentation), however, describe well the spectral shapes of Ξ and Ω baryons and their multiplicity dependence. Since the total particle yield contains contributions from soft and hard particle production, which cannot be experimentally separated, we argue that the correct description of the p_T -spectra is a minimum requirement for meaningful comparisons of multiplicity dependent yield measurements to MPI based calculations. We demonstrate that the s -fragmentation component describes the increase of average p_T and yields with multiplicity seen in the data, including the approximate multiplicity scaling for different collision energies. When restricted to processes that reproduce the measured p_T -spectra, the MPI framework exhibits a smooth evolution from strictly proportional multiplicity scaling (K_S^0 , Λ , where the udg -hadronization component dominates) to linearity (s -fragmentation) and on to increasingly non-linear behavior (c -, b -quark and high- p_T jet fragmentation), hence providing a unified approach for particle production across all particle species in pp collisions.

One of the pillars of the high-energy ultra-relativistic heavy-ion physics program is to study the evolution and onset of potential quark-gluon plasma (QGP) phenomena in smaller collision systems like pp and pA collisions at RHIC and LHC collision energies [1]. In high-energy pp collisions at the LHC, the integrated yields of strange and multi-strange particles relative to pions were reported to increase significantly with the event multiplicity, reaching values similar to those in pPb and PbPb collisions [2]. Strangeness enhancement was originally proposed as a signature of QGP formation in nuclear collisions [3]. In the picture of statistical hadronization, the increase with multiplicity in smaller systems, which is rather independent of collision species and energy [4, 5], is a result of decreasing canonical suppression [6] towards the grand-canonical ensemble realized in more central PbPb collisions [7, 8]. The strangeness data together with other measurements in high-multiplicity pp collisions, in particular the ridge [9, 10], resemble collective properties as found in heavy-ion collisions and provoke speculation about the formation of a QGP in these collisions [1, 11]. Indeed, models incorporating final-state interactions originally developed for heavy-ion collisions, are also able to describe the pp data [12–15]. Refined models based on the “core/corona” approach, where the core of the collisions is assumed to “hydrodynamize”, while the corona is treated as a superposition of independent nucleon–nucleon collision, achieve a good description of data across all systems with a rather universal approach [16, 17].

In this paper, we focus on an alternative description of the pp data [2, 5] based on the MPI model, as implemented in the PYTHIA event generator [18]. Unlike other works [19–21], we rely on the original string fragmentation, but include coherence effects between multiple scatterings (e.g. color reconnection [22, 23]). We discuss the qualitative expectations of the model for multiplicity dependent measurements as well as the possible effects that can explain strangeness enhancement in pp collisions. An important ingredient for the MPI model is the pp impact parameter (b) dependence of the number of MPI (N_{mpi}), which was originally introduced for an accurate description of the dispersion of multiplicity distributions and the pedestal effect in underlying event measurements [24]. More recently it has been shown that the pp impact parameter dependence is also important for understanding the centrality dependence of hard processes in pPb [25, 26] and peripheral PbPb collisions [27]. In both cases a detailed study of possible nucleon–nucleon impact parameter biases was triggered by unexpected deviations from the number of binary collisions (N_{coll}) scaling. In pp collisions, an equivalent scaling factor would be N_{mpi} , however at present it cannot be extracted from data. Hence, in the absence of a standard scaling expectation, one has to be particularly careful with the interpretation of multiplicity-dependent mea-

surements in pp collisions.

Assuming that a pp event can be described by a superposition of independent parton–parton scatterings, it is reasonable to expect that particle multiplicity is approximately proportional to N_{mpi} . For central collisions ($b = 0$), N_{mpi} reaches about 3.5 times the value of N_{mpi} averaged over all impact parameters. Higher values are only accessed by rather improbable statistical (e.g. Poissonian) fluctuations. Hence, one can expect a roughly linear dependence between multiplicity and N_{mpi} until 3.5 times the mean multiplicity, above which multiplicity fluctuations and not impact parameter variations dominate particle production. In such a model, both the yields of soft particles and those related to hard scatterings would be proportional to the event multiplicity over a wide range of multiplicities. However, one can expect important differences at low and high multiplicities for the following reasons:

1. Particles originating from hard scatterings have associated particle production contributing to the event multiplicity both close to the scattered particle in azimuth (φ) and pseudorapidity (η) (near-side) and back-to-back ($\varphi \approx \pi$) over a wide η -range. Particles are also produced from the fragmentation of strings spanned between partons and the beam remnants, also over a wide η -range. The near-side contribution can be experimentally excluded by measuring the multiplicity in an η -region well separated from the region in which the signal particle yield is measured [28].
2. Low-multiplicity events have a large contribution from soft collisions in which no hard scatterings occur and also from the soft underlying event.

Associated particle production can lead to a stronger than linear increase of yields (auto-correlation bias) at high multiplicities (above 3.5 times the average multiplicity) where multiplicity fluctuations dominate. Both effects mentioned above lead to a threshold multiplicity above which a proportionality between yields and multiplicity sets in.

Indeed, as demonstrated by the straight-line fits in Fig. 1, the measured yields of strange particles have an approximate linear dependence on the charged-particle multiplicity, but only above some minimum multiplicity (M_0). The multiplicity reaches 3.5 (3.8) times the minimum bias multiplicity for $\sqrt{s} = 7$ TeV (13 TeV), i.e. within the expected range of proportionality. The intercept increases with mass and strangeness, indicative of a higher importance of hard processes for multi-strange baryon production.

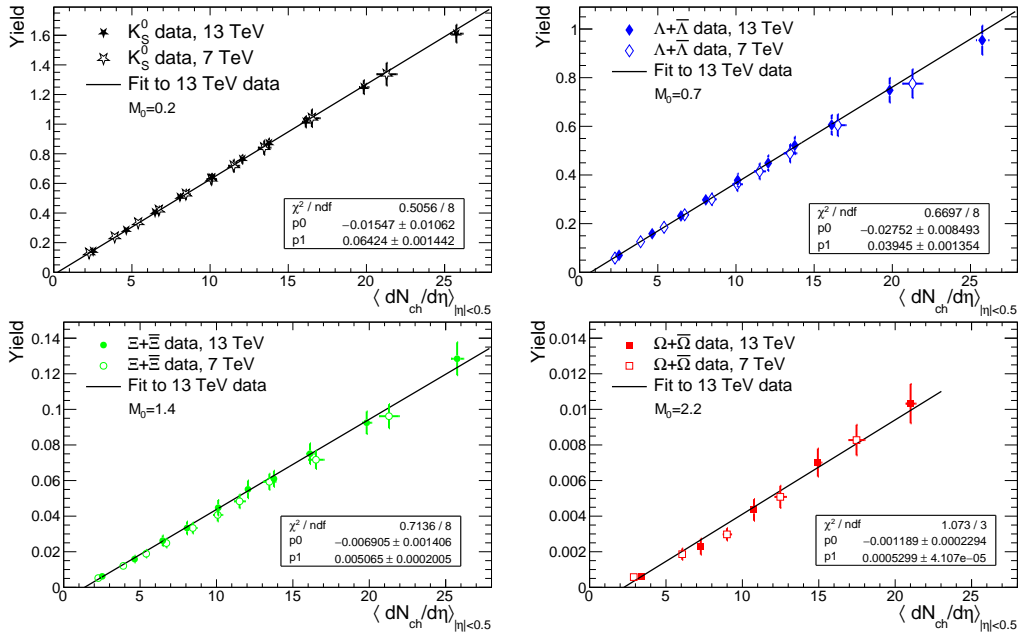


Figure 1: Measured yields of strange particles (K_S^0 , Λ , Ξ , Ω) versus charged-particle multiplicity at midrapidity ($|\eta| < 0.5$) in pp collisions at $\sqrt{s} = 7$ and 13 TeV [2, 5]. A straight-line fit to the 13 TeV data is shown in each case.

Using the intercept, the functional relation of the yields on multiplicity can be expressed as $\propto (M - M_0)$.¹

The reported strangeness enhancement [2, 5] is reproduced in Fig. 2 by normalizing the strange particle yields with the charged-particle multiplicity (as a proxy for the charged-pion yields). Due to the normalization, which is $\propto M$ trivially, the resulting functional dependence is $\propto (1 - M_0/M)$, i.e. a hyperbolic decrease with multiplicity towards the intercept, which leads to a rise with M that is most apparent at low multiplicities. However, the rise is still visible above the mean multiplicity ($dN/d\eta = 6.9$) leading to the impression of an enhancement effect. Hence, in the original MPI picture, the data can be interpreted to result from a minimum associated multiplicity necessary for multi-strange particle production and/or different scaling of soft and (semi-)hard processes, i.e. a single string effect leading to suppression at low

¹Here and in the following the charged-particle multiplicity is always expressed as average charged-particle pseudorapidity density at midrapidity, i.e. $\langle dN/d\eta \rangle_{|\eta|<0.5}$, in event classes which were obtained by dividing the multiplicity distributions measured or calculated with the PYTHIA generator in the forward ranges of $-3.7 < \eta < -1.7$ and $2.8 < \eta < 5.1$ (ALICE V0 detector acceptance) to suppress the auto-correlation bias.

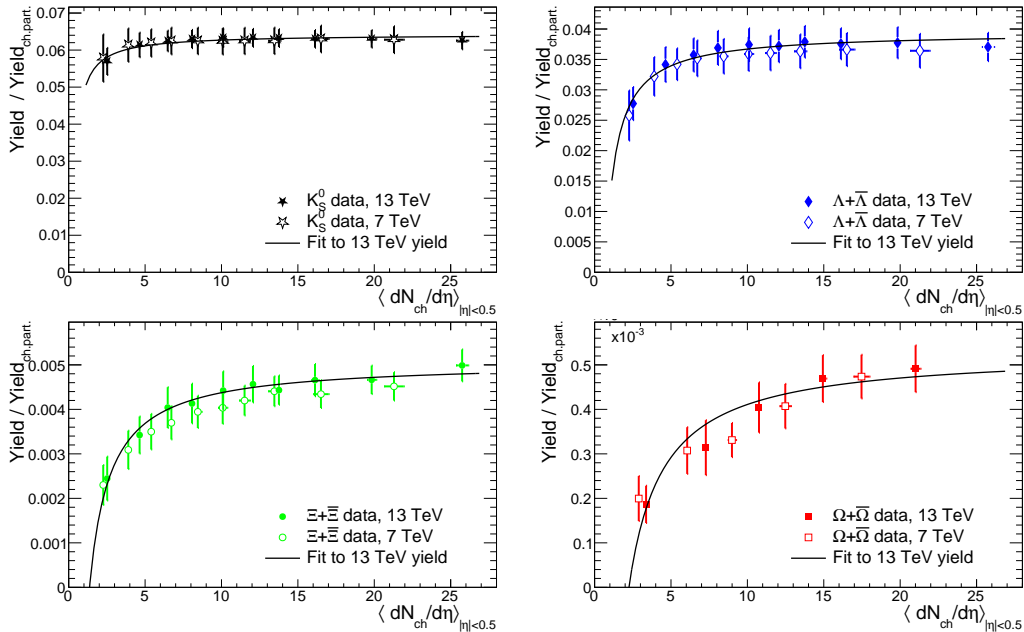


Figure 2: Same data and fits as in Fig. 1, except that both data and fits were normalized by the charged-particle multiplicity at midrapidity ($|\eta| < 0.5$) (i.e., normalized by the x -axis values).

multiplicity that is reduced at higher multiplicity.

However, the PYTHIA generator, in its original form, does not describe the strangeness data, and does not even exhibit a rising trend of the strange particle yield ratios with multiplicity (see Fig. 2 in [2]). This is in particular surprising because it generally describes the multiplicity-dependence of particle production at high p_T well (see for e.g. [30]).

For light-flavor particle yield measurements, it is experimentally challenging, if not impossible, to separate the yields into soft and hard production based on p_T . Hence, it is a minimum requirement for meaningful comparisons of multiplicity dependent yield measurements to MC calculations, that the corresponding p_T spectra are well described. However, Ξ and Ω baryon production measured above a p_T of about 1 GeV/ c in pp collisions at 7 TeV, is significantly harder (by factor 2–4) above 2 GeV/ c in data compared to PYTHIA calculations (see Fig. 2 in [31]). Hence, in Fig. 3 we compare Ξ^- spectra in non-single diffractive pp collisions at 0.9 and 7 TeV, which were measured by CMS [29] down to nearly zero p_T , with calculations of PYTHIA 6 (Perugia 2011 tune [32]). The calculated spectrum, which is normalized to the data for $p_T > 2$ GeV/ c , is found to well describe the measured

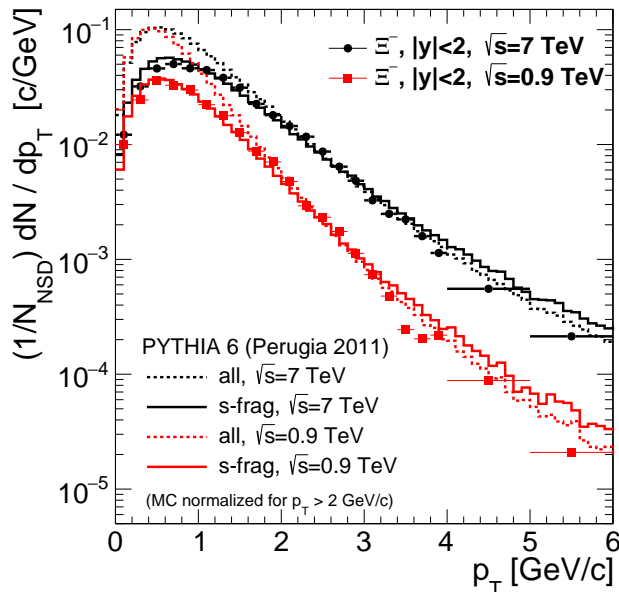


Figure 3: Ξ^- spectra in pp collisions at 0.9 and 7 TeV measured by CMS [29] down to nearly zero p_T compared with PYTHIA 6 (Perugia 2011) calculations. The calculated spectra, which are shown for all produced Ξ^- as well as for those produced by s-quark fragmentation alone, are normalized to the data in the region $p_T > 2$ GeV/c.

spectral shape at high- p_T , but significantly overshoots the data at low p_T . To understand the low- p_T excess in PYTHIA, we separate the produced strange particles into two categories: These are strange particles that result from string fragmentation of a string containing:

- only u -quarks, d -quarks or gluons, called “ udg -hadronization”;
- at least one s -quark produced by flavor creation or excitation in the parton shower, called “ s -fragmentation”.

As can be seen in Fig. 3, the spectra of Ξ^- produced by s -quark fragmentation alone in PYTHIA well describe the spectral shape of the data, even down to low p_T . In general, particle production by udg -hadronization dominates the PYTHIA calculation, in particular of course for the soft component. In the normalization region (above 2 GeV/c), the yield produced by s -fragmentation is about half of the total calculated yield.

In Fig. 4, we compare calculated spectra using PYTHIA 6 (Perugia 2011) with the measured p_T -spectra (K_S^0 , Λ , Ξ , Ω) in low, medium and high multiplicity pp collisions at $\sqrt{s} = 13$ TeV. As before, the calculated spectra

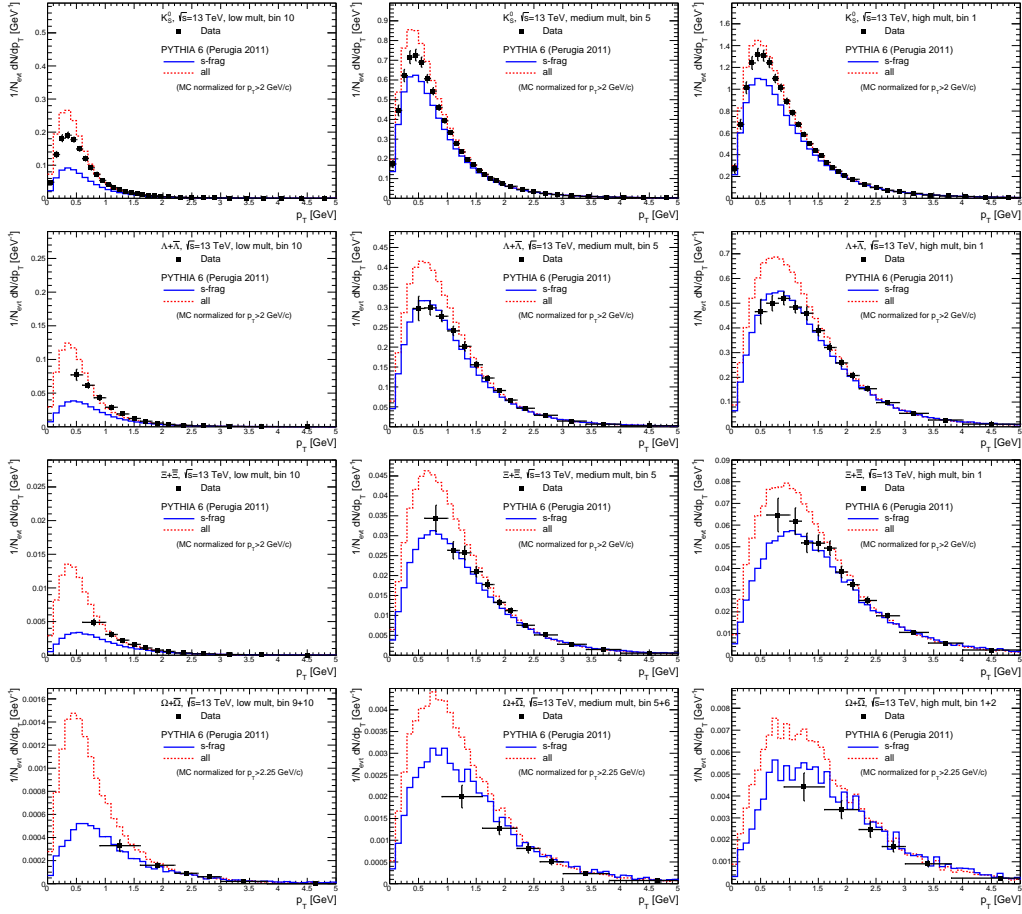


Figure 4: Strange particle p_T -spectra (K_S^0 , Λ , Ξ , Ω) measured in low (left panels), medium (middle panels) and high (right panels) multiplicity pp collisions at $\sqrt{s} = 13$ by ALICE TeV [5] compared with PYTHIA 6 (Perugia 2011) calculations. The calculated distributions, which show all produced particles of a given type, as well as those produced by s -quark fragmentation alone, are normalized to the data in the region $p_T \gtrsim 2$ GeV/ c .

are normalized to the data in the region $p_T \gtrsim 2$ GeV/ c . In data, the soft component appears in particular for the low-multiplicity interval as well as for the K^0 , while otherwise the spectral shapes are well described by the s -fragmentation component.

In Fig. 5, we compare the measured $\langle p_T \rangle$ of strange particles (K_S^0 , Λ , Ξ , Ω) versus multiplicity in pp collisions at $\sqrt{s} = 13$ TeV [5] with calculations of PYTHIA 6 (Perugia 2011). As expected from the comparison of the p_T -spectra, the data are generally well reproduced by the calculations using

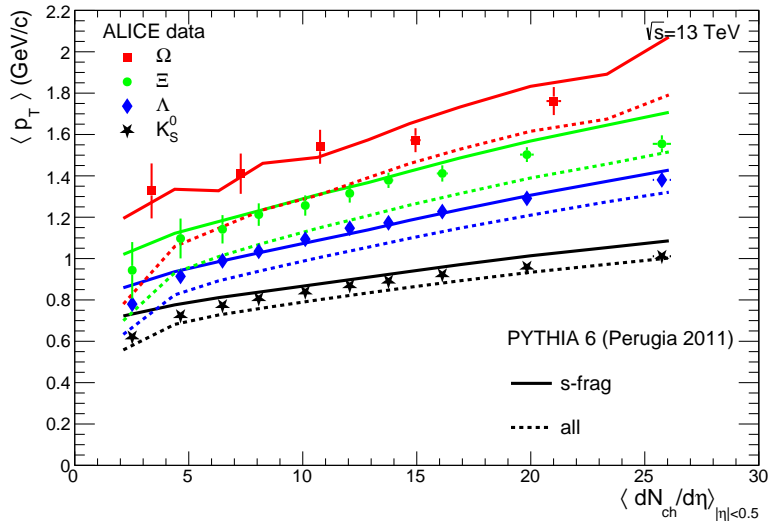


Figure 5: Average transverse momenta of strange particles (K_S^0 , Λ , Ξ , Ω) versus charged-particle multiplicity at midrapidity in pp collisions at $\sqrt{s} = 13$ TeV measured by ALICE [5] compared with PYTHIA 6 (Perugia 2011) calculations. The calculation shows the $\langle p_T \rangle$ of all produced particles of a given type, as well as the $\langle p_T \rangle$ of those produced by s -quark fragmentation alone.

s -quark fragmentation alone, except in the case of the K_S^0 .

Since the absolute yield is typically not well reproduced in calculations, we compare the self-normalized yields (i.e. the yield in a given multiplicity interval normalized to its average yield) as a function of multiplicity, in Fig. 6, between data and PYTHIA 6 (Perugia 2011) calculations. The self-normalized yields for all produced particles which are dominated by udg -hadronization and by s -quark fragmentation alone enclose the data points. The udg -dominated yields pass through (0,0) while the s -fragmentation component has a finite intercept with the x -axis. The comparison of the data with the calculations suggests that the K_S^0 and Λ yields are dominated by udg -hadronization, while Ξ and Ω yields by s -fragmentation. The production of Λ particles may also have a sizeable contribution from the s -fragmentation component. However, these interpretations rely on the shape of the p_T -spectra as modelled by PYTHIA. It cannot be excluded that the udg -hadronization dynamics for multi-strange baryons is not implemented correctly and that with a correct implementations both mechanisms would show the threshold behavior. A way to avoid the interference of the soft and semi-hard components is to compare to self-normalized strange-particle yields extracted above

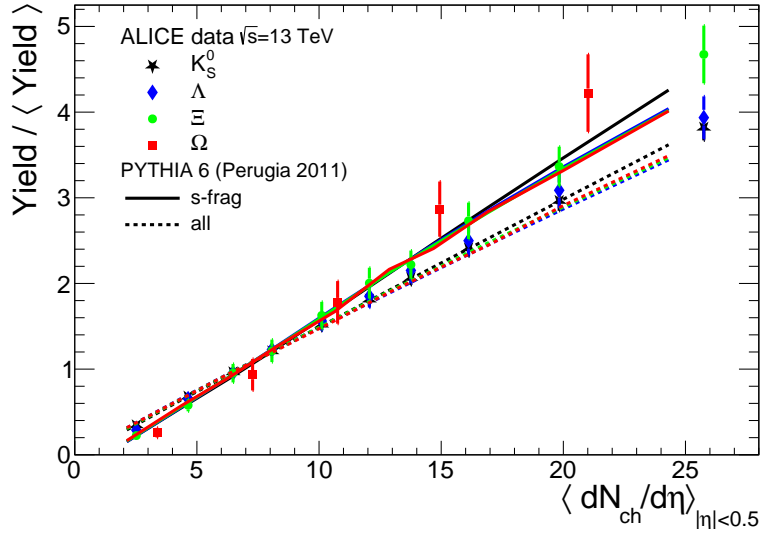


Figure 6: Self-normalized yields of strange particles (K_S^0 , Λ , Ξ , Ω) versus charged-particle multiplicity at midrapidity in pp collisions at $\sqrt{s} = 13$ TeV [5] compared with PYTHIA 6 (Perugia 2011) calculations. The calculation shows the yield of all produced particles of a given type, as well as the yield of those produced by s -quark fragmentation alone.

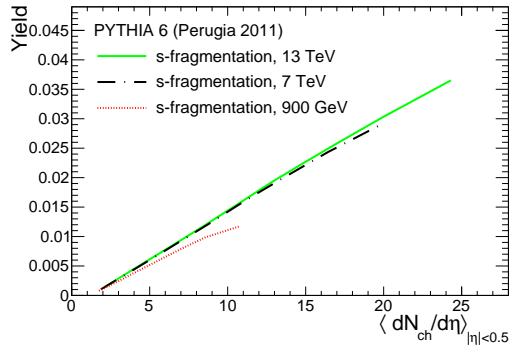


Figure 7: Comparison of Ξ yield versus charged-particle multiplicity at midrapidity in pp collisions at $\sqrt{s} = 0.9, 7$ and 13 TeV for s -quark fragmentation computed with PYTHIA 6 (Perugia 2011).

a certain p_T threshold (Fig. 6 of [5]), which were found to be well described by PYTHIA.

The \sqrt{s} -independence of the strange-particle yields versus multiplicity between $\sqrt{s} = 7$ and 13 TeV (see Fig. 1 and Fig. 2) is reproduced in PYTHIA

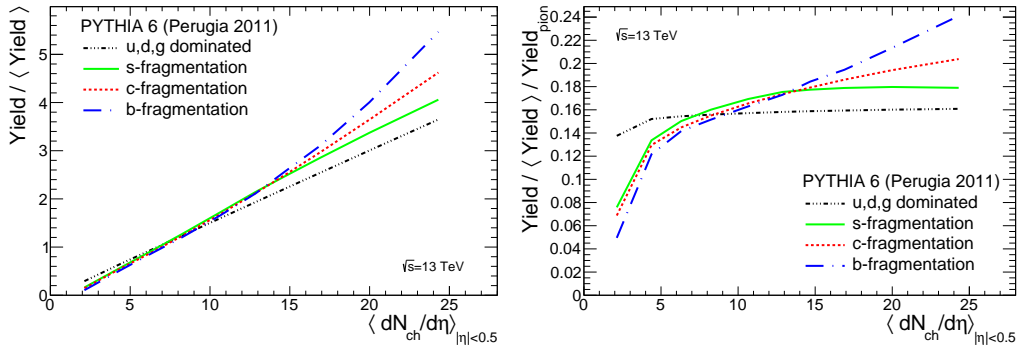


Figure 8: Left: Self-normalized yields versus charged-particle multiplicity at midrapidity in pp collisions at $\sqrt{s} = 13$ TeV for different flavors computed with PYTHIA 6 (Perugia 2011). Right: Same as on the left panel, except that the yields are further normalized by the charged pion yield.

as shown in Fig. 7. Hence, “multiplicity scaling” in-itself cannot be interpreted as a consequence of final state effects. A significant deviation from this scaling is, however, expected at lower energies ($\sqrt{s} = 900$ GeV in Fig. 2). The reason is that the number of charged particles produced per MPI decreases only logarithmically with \sqrt{s} .

The quark-flavor evolution of both the self-normalized yields and self-normalized yields per charged-pion yields computed with PYTHIA 6 (Perugia 2011) are shown in Fig. 8. A smooth transition from linear to quadratic dependence from the udg -hadronization and s -fragmentation components to c - and b -fragmentation components emerges, which in the MPI picture, results as a consequence of the significant contribution of associated particle production to the measured multiplicity (auto-correlation bias) [28].

In order to elucidate the origin of the multiplicity threshold we investigate the effect from three different angles:

i) In the left panel of Fig. 9 we compare the N_{mpi} probability distribution for Ξ baryons from (u, d, g) -hadronization to the those for s -fragmentation. Both processes bias the N_{mpi} -distribution towards the “fully biased” distribution expected for rare processes. However, the s -fragmentation tag biases the MPI distribution to higher values, i.e. more central collisions, compared to (u, d, g) -hadronization. The difference is particularly important below the unbiased (minimum-bias) average N_{mpi} of 3.2 corresponding to the lowest multiplicity bins in data. It results from the presence of double-diffractive collisions which have $N_{\text{mpi}} = 0$ (only seen for (u, d, g) -hadronization) and an important contribution to soft particle production in peripheral collisions.

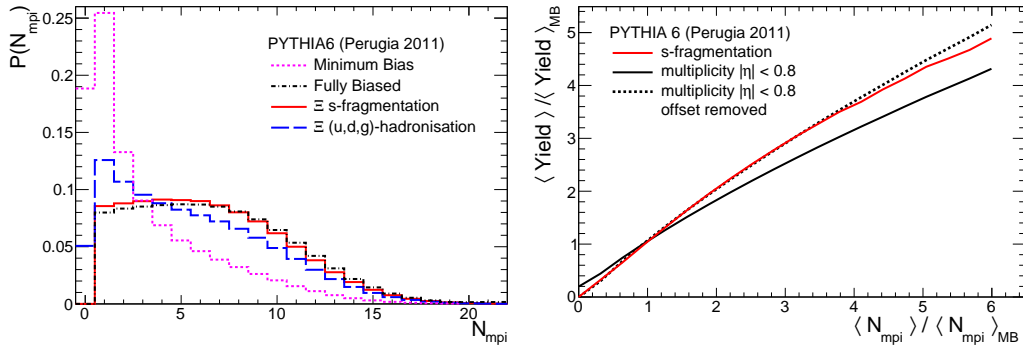


Figure 9: Left: The MPI probability distribution for Ξ baryons from (u, d, g) -hadronization (long-dashed blue) is compared to the one from s -fragmentation (solid red). As references we show also the minimum-bias distribution (fine-dashed) and the fully biased distributions ($N_{\text{mpi}} P_{\text{MinBias}}(N_{\text{mpi}})$) expected for hard processes (short-long dashed black). Right: Self-normalised Ξ yields from s -fragmentation (red) and charged particle multiplicity (black solid) as a function of the self-normalised number of MPI. The dotted line shows the multiplicity with the soft contribution ($N_{\text{mpi}} = 0$) removed.

Note that this interpretation is further corroborated by the shape of the multiplicity dependence of the average p_T at low multiplicity (Fig. 5, "ledge effect" [33]).

ii) In the right panel of Fig. 9 we show the self-normalised yield of Ξ baryons from s -fragmentation versus the self-normalised number of MPIs and compare it to the self-normalised multiplicity versus the same quantity. While s -fragmentation exhibits a strict proportionality at low N_{mpi} , charged particle multiplicity stays finite down to $N_{\text{mpi}} = 0$. The reason is that multiplicity also receives contributions from soft processes. If one subtracts this soft offset the multiplicity follows the s -fragmentation yield over a wide range of N_{mpi} which explains the linear behaviour of s -fragmentation versus multiplicity above the threshold. In particular, the weaker than linear increase at higher N_{mpi} results in PYTHIA from color-reconnection and affects multiplicity and s -fragmentation almost equally.

iii) In order to remove the centrality bias we compare in the left panel of Fig. 10, for a fixed $N_{\text{mpi}} = 1$, the charged particle pseudorapidity density for events with a Ξ from (u, d, g) -hadronization at midrapidity to the one for s -fragmentation tagged events. For s -fragmentation the density is about 0.2 units higher. The difference is also reflected in the azimuthal angle dis-

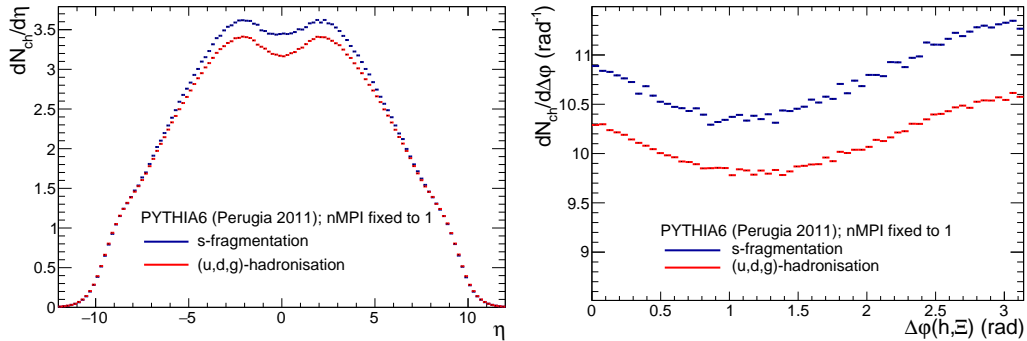


Figure 10: Left: For a fixed $N_{\text{mpi}} = 1$, the charged particle pseudorapidity density for events with a Ξ (u, d, g)-hadronization at midrapidity (blue) is compared to the one for s -fragmentation tagged events (red). Right: The corresponding azimuth angle difference distribution between charged hadrons and the Ξ for $|\eta| < 5$.

tribution between charged hadrons and the Ξ baryon with a slightly more pronounced back-to-back structure for s -fragmentation (Fig. 10(right)).

In summary, motivated by the importance of modelling the pp impact parameter dependency of MPIs for the understanding of not only the multiplicity dispersion, underlying event properties and multiplicity dependence of hard processes in pp but also the centrality dependence of hard processes in pPb and peripheral PbPb collisions, we investigated whether strangeness enhancement in pp collisions at the LHC can be understood within the original MPI picture implemented in the PYTHIA event generator. We started by showing that the measured yields can be parameterized by straight-line fits, where the intercept increases with increasing strangeness and mass of the particle (Fig. 1). Normalizing the strange-particle yields by the charged-particle multiplicity leads to a hyperbolic decrease with multiplicity towards the intercept (Fig. 2), which in the original MPI picture is naturally explained as a suppression of strange-particle yields at low multiplicity that is reduced for higher multiplicities. By comparing PYTHIA 6 (Perugia 2011) calculations with data down to low p_T (Fig. 3) and in intervals of multiplicity (Fig. 4), we argued that the strangeness enhancement in PYTHIA is masked by a large excess of soft baryons, which largely results from the hadronization of u quark, d quark and gluon strings. At higher p_T , strings formed from parton showers initiated by strange quarks describe the spectral shape of Ξ and Ω baryons well. Furthermore, we demonstrate that the s -fragmentation component exhibits the transverse momentum (Fig. 5)

and yield enhancements (Fig. 6) seen in the data, including the approximate multiplicity scaling for different collision energies (Fig. 7). This suggests that s -quark fragmentation plays a dominant role for the production of these baryons. However, we cannot exclude that a (udg) -hadronization implementation which reproduces the p_T -spectra could also describe the enhancement. The MPI framework exhibits a smooth evolution (Fig. 8) from strict-proportional multiplicity scaling (K_S^0 , Λ where the udg -hadronization component dominates) to linearity (Ξ , Ω where s -fragmentation dominates) and on to increasingly non-linear behavior (c and b quark fragmentation as well as high- p_T particles), and hence provides a unified approach for particle production across all particle species in pp collisions. In PYTHIA, the multiplicity threshold for s -fragmentation has two origins: i) a bias towards more central collisions compared to yields which also receive contributions from soft processes (Fig. 9) ii) for a fixed centrality (in particular for low-multiplicity peripheral collisions) particle production is correlated with multi-strange baryons (Fig. 10). The centrality difference originates from the presence of double-diffractive collisions and an important contribution to soft particle production in peripheral collisions.

While all calculations for the paper were made with PYTHIA 6 (Perugia 2011) the same qualitative and mostly also the same quantitative description was found with PYTHIA 8 (Monash) (as shown in the appendix A). In appendix B we additionally show that, as expected by the authors, the current implementation of rope hadronization introduced in [34] does not describe the mean p_T . Note that this observation is at variance with the claims in [21]. We stress that while the multiplicity-dependencies of the measured strange-particle yields are described, their absolute yields are significantly underestimated within the original PYTHIA model. Further insight in to the interplay of the underlying particle production mechanisms can be expected from two-particle angular correlation measurements between strange and (non-)strange particles. These and other studies, in particular when they involve the Ω baryon, will greatly benefit from the large increase in the number of events provided by the 200/pb pp program planned for Run-3/4 at the LHC [35].

We thank J. Schukraft for many fruitful discussions on this topic over the past years and C. Bierlich for providing information on the rope hadronisation implementation in PYTHIA 8. We also thank S. Dash and R. Nayak for making available the PYTHIA 8 settings used in [21] and N. Zardoshti for the proofreading of the manuscript. C.L. acknowledges financial support by the U.S. Department of Energy, Office of Science, Office of Nuclear Physics, under contract number DE-AC05-00OR22725.

References

- [1] J. L. Nagle and W. A. Zajc, “Small system collectivity in relativistic hadronic and nuclear collisions,” *Ann. Rev. Nucl. Part. Sci.* **68** (2018) 211–235, [arXiv:1801.03477 \[nucl-ex\]](#).
- [2] **ALICE** Collaboration, J. Adam *et al.*, “Enhanced production of multi-strange hadrons in high-multiplicity proton-proton collisions,” *Nature Phys.* **13** (2017) 535–539, [arXiv:1606.07424 \[nucl-ex\]](#).
- [3] P. Koch, B. Müller, and J. Rafelski, “Strangeness in relativistic heavy ion collisions,” *Phys. Rept.* **142** (1986) 167–262.
- [4] **ALICE** Collaboration, S. Acharya *et al.*, “Multiplicity dependence of light-flavor hadron production in pp collisions at $\sqrt{s} = 7$ TeV,” *Phys. Rev. C* **99** no. 2, (2019) 024906, [arXiv:1807.11321 \[nucl-ex\]](#).
- [5] **ALICE** Collaboration, S. Acharya *et al.*, “Multiplicity dependence of (multi-)strange hadron production in proton–proton collisions at $\sqrt{s} = 13$ TeV,” *Eur. Phys. J. C* **80** no. 2, (2020) 167, [arXiv:1908.01861 \[nucl-ex\]](#).
- [6] V. Viskovic and A. Kalweit, “Multiplicity dependence of light flavour hadron production at LHC energies in the strangeness canonical suppression picture,” [arXiv:1610.03001 \[nucl-ex\]](#).
- [7] **ALICE** Collaboration, B. B. Abelev *et al.*, “Multi-strange baryon production at mid-rapidity in PbPb collisions at $\sqrt{s_{NN}} = 2.76$ TeV,” *Phys. Lett.* **B728** (2014) 216–227, [arXiv:1307.5543 \[nucl-ex\]](#). [Erratum: *Phys. Lett.*B734,409(2014)].
- [8] N. Sharma, J. Cleymans, B. Hippolyte, and M. Paradza, “A Comparison of pp pPb, PbPb collisions in the thermal model: Multiplicity dependence of thermal parameters,” *Phys. Rev. C* **99** no. 4, (2019) 044914, [arXiv:1811.00399 \[hep-ph\]](#).
- [9] **CMS** Collaboration, V. Khachatryan *et al.*, “Observation of long-range near-side angular correlations in proton–proton collisions at the LHC,” *JHEP* **09** (2010) 091, [arXiv:1009.4122 \[hep-ex\]](#).
- [10] **CMS** Collaboration, V. Khachatryan *et al.*, “Evidence for collectivity in pp collisions at the LHC,” *Phys. Lett. B* **765** (2017) 193–220, [arXiv:1606.06198 \[nucl-ex\]](#).

- [11] C. Loizides, “Experimental overview on small collision systems at the LHC,” *Nucl. Phys.* **A956** (2016) 200–207, [arXiv:1602.09138](#) [nucl-ex].
- [12] M. Habich, G. A. Miller, P. Romatschke, and W. Xiang, “Testing hydrodynamic descriptions of pp collisions at $\sqrt{s} = 7$ TeV,” *Eur. Phys. J. C* **76** no. 7, (2016) 408, [arXiv:1512.05354](#) [nucl-th].
- [13] R. D. Weller and P. Romatschke, “One fluid to rule them all: viscous hydrodynamic description of event-by-event central pp, pPb and PbPb collisions at $\sqrt{s} = 5.02$ TeV,” *Phys. Lett. B* **774** (2017) 351–356, [arXiv:1701.07145](#) [nucl-th].
- [14] D. K. Srivastava, R. Chatterjee, and S. A. Bass, “Transport dynamics of parton interactions in pp collisions at energies available at the CERN Large Hadron Collider,” *Phys. Rev. C* **97** no. 6, (2018) 064910, [arXiv:1801.07482](#) [nucl-th].
- [15] T. Shao, J. Chen, C. M. Ko, and Z.-W. Lin, “Enhanced production of strange baryons in high-energy nuclear collisions from a multiphase transport model,” *Phys. Rev. C* **102** no. 1, (2020) 014906, [arXiv:2012.10037](#) [nucl-th].
- [16] T. Pierog, I. Karpenko, J. M. Katzy, E. Yatsenko, and K. Werner, “EPOS LHC: Test of collective hadronization with data measured at the CERN Large Hadron Collider,” *Phys. Rev. C* **92** no. 3, (2015) 034906, [arXiv:1306.0121](#) [hep-ph].
- [17] Y. Kanakubo, Y. Tachibana, and T. Hirano, “Unified description of hadron yield ratios from dynamical core-corona initialization,” *Phys. Rev. C* **101** no. 2, (2020) 024912, [arXiv:1910.10556](#) [nucl-th].
- [18] T. Sjostrand, S. Mrenna, and P. Z. Skands, “PYTHIA 6.4 Physics and Manual,” *JHEP* **05** (2006) 026, [arXiv:hep-ph/0603175](#) [hep-ph].
- [19] N. Fischer and T. Sjöstrand, “Thermodynamical string fragmentation,” *JHEP* **01** (2017) 140, [arXiv:1610.09818](#) [hep-ph].
- [20] H. J. Pirner, B. Z. Kopeliovich, and K. Reygers, “Strangeness enhancement due to string fluctuations,” *Phys. Rev. D* **101** no. 11, (2020) 114010, [arXiv:1810.04736](#) [hep-ph].
- [21] R. Nayak, S. Pal, and S. Dash, “Effect of rope hadronization on strangeness enhancement in pp collisions at LHC energies,” *Phys. Rev. D* **100** no. 7, (2019) 074023, [arXiv:1812.07718](#) [hep-ph].

- [22] R. Corke and T. Sjostrand, “Interleaved parton showers and tuning prospects,” *JHEP* **03** (2011) 032, [arXiv:1011.1759 \[hep-ph\]](#).
- [23] C. Bierlich and J. R. Christiansen, “Effects of color reconnection on hadron flavor observables,” *Phys. Rev. D* **92** no. 9, (2015) 094010, [arXiv:1507.02091 \[hep-ph\]](#).
- [24] T. Sjostrand and M. van Zijl, “Multiple parton–parton interactions in an impact parameter picture,” *Phys. Lett.* **B188** (1987) 149–154.
- [25] **ALICE** Collaboration, A. Morsch, “pPb results from ALICE with an emphasis on centrality determination,” *J. Phys. Conf. Ser.* **509** (2014) 012021, [arXiv:1309.5525 \[nucl-ex\]](#).
- [26] **ALICE** Collaboration, J. Adam *et al.*, “Centrality dependence of particle production in pPb collisions at $\sqrt{s_{NN}}=5.02$ TeV,” *Phys. Rev. C* **91** no. 6, (2015) 064905, [arXiv:1412.6828 \[nucl-ex\]](#).
- [27] C. Loizides and A. Morsch, “Absence of jet quenching in peripheral nucleu–nucleus collisions,” *Phys. Lett. B* **773** (2017) 408–411, [arXiv:1705.08856 \[nucl-ex\]](#).
- [28] S. G. Weber, A. Dubla, A. Andronic, and A. Morsch, “Elucidating the multiplicity dependence of J/ψ production in proton–proton collisions with PYTHIA8,” *Eur. Phys. J. C* **79** no. 1, (2019) 36, [arXiv:1811.07744 \[nucl-th\]](#).
- [29] **CMS** Collaboration, V. Khachatryan *et al.*, “Strange particle production in pp collisions at $\sqrt{s} = 0.9$ and 7 TeV,” *JHEP* **05** (2011) 064, [arXiv:1102.4282 \[hep-ex\]](#).
- [30] **ALICE** Collaboration, S. Acharya *et al.*, “Charged-particle production as a function of multiplicity and transverse sphericity in pp collisions at $\sqrt{s} = 5.02$ and 13 TeV,” *Eur. Phys. J. C* **79** no. 10, (2019) 857, [arXiv:1905.07208 \[nucl-ex\]](#).
- [31] **ALICE** Collaboration, B. Abelev *et al.*, “Multi-strange baryon production in pp collisions at $\sqrt{s} = 7$ TeV with ALICE,” *Phys. Lett. B* **712** (2012) 309–318, [arXiv:1204.0282 \[nucl-ex\]](#).
- [32] P. Z. Skands, “Tuning Monte Carlo generators: The Perugia tunes,” *Phys. Rev. D* **82** (2010) 074018, [arXiv:1005.3457 \[hep-ph\]](#).

- [33] X.-N. Wang and R. C. Hwa, “The effect of jet production on the multiplicity dependence of average transverse momentum,” *Phys. Rev. D* **39** (1989) 187.
- [34] C. Bierlich, G. Gustafson, L. Lönnblad, and A. Tarasov, “Effects of overlapping strings in pp collisions,” *JHEP* **03** (2015) 148, [arXiv:1412.6259 \[hep-ph\]](#).
- [35] Z. Citron *et al.*, “Report from Working Group 5: Future physics opportunities for high-density QCD at the LHC with heavy-ion and proton beams,” *CERN Yellow Rep. Monogr.* **7** (2019) 1159–1410, [arXiv:1812.06772 \[hep-ph\]](#).

Appendix

A Additional figures

We show here the figures Fig. 11, Fig. 12, Fig. 13 and Fig. 14 which were obtained with PYTHIA 8 (Monash) instead of PYTHIA 6 (Perugia 2011). For PYTHIA 6 we used version 6.4.25, while for PYTHIA 8, version 8.243. We checked that we get the same results for PYTHIA 8 with the latest version 8.306.

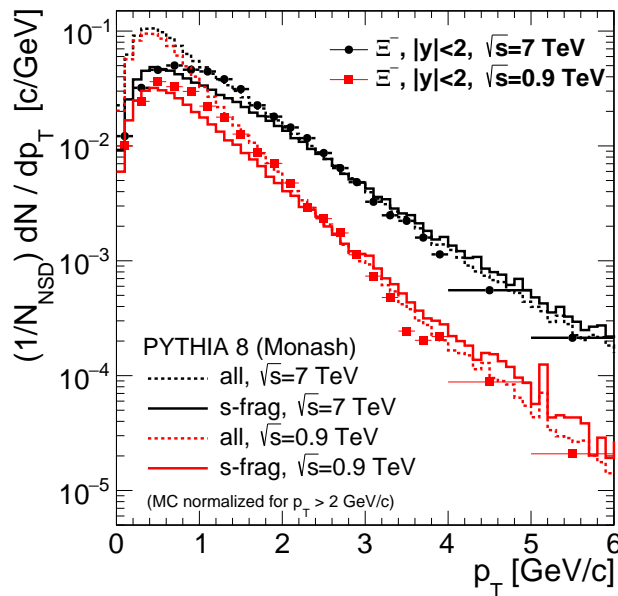


Figure 11: Ξ^- spectra in pp collisions at 0.9 and 7 TeV measured by CMS [29] down to nearly zero p_T compared with PYTHIA 8 (Monash) calculations. The calculated spectra, which are shown for all produced Ξ^- as well as for those produced by s-quark fragmentation alone, are normalized to the data in the region $p_T > 2$ GeV/c. See Fig. 3 for the corresponding PYTHIA 6 (Perugia 2011) calculations.

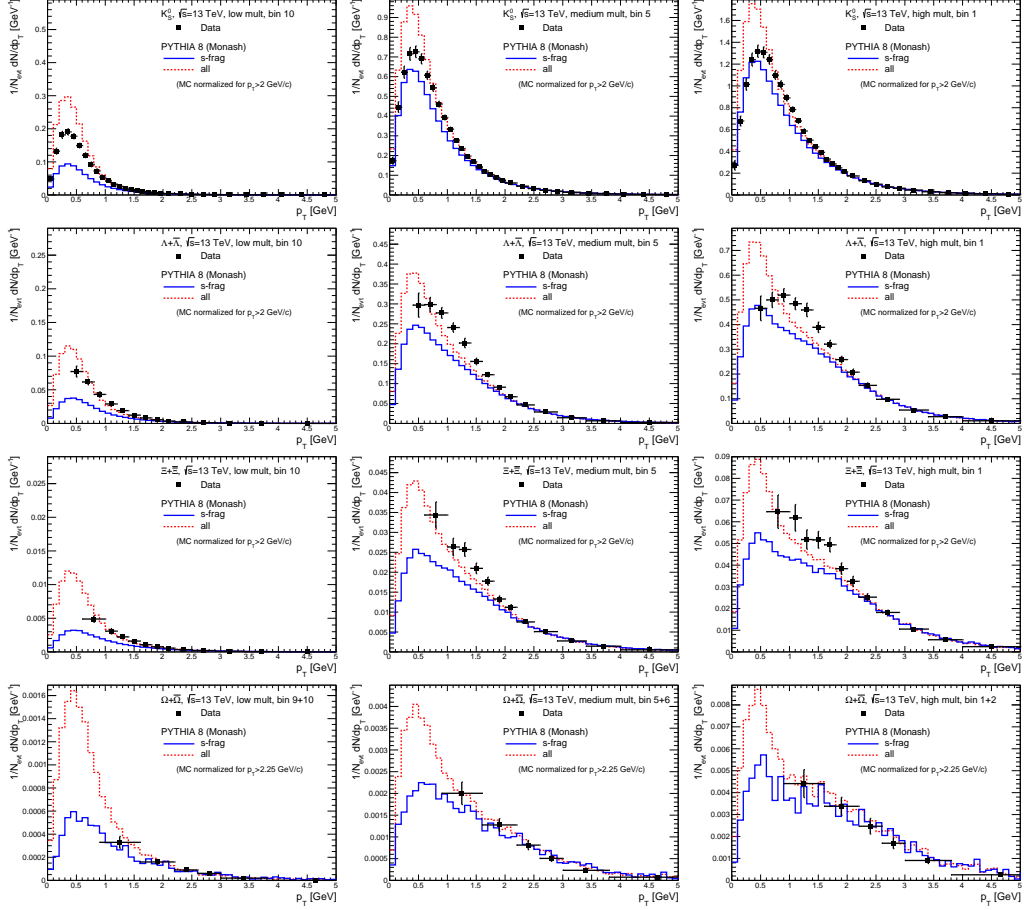


Figure 12: Strange particle p_T -spectra (K_S^0 , Λ , Ξ , Ω) measured in low (left panels), medium (middle panels) and high (right panels) multiplicity pp collisions at $\sqrt{s} = 13$ TeV [5] compared with PYTHIA 8 (Monash) calculations. The calculated distributions, which show all produced particles of a given type, as well as those produced by s -quark fragmentation alone, are normalized to the data in the region $p_T \gtrsim 2$ GeV/ c . See Fig. 4 for the corresponding PYTHIA 6 (Perugia 2011) calculations.

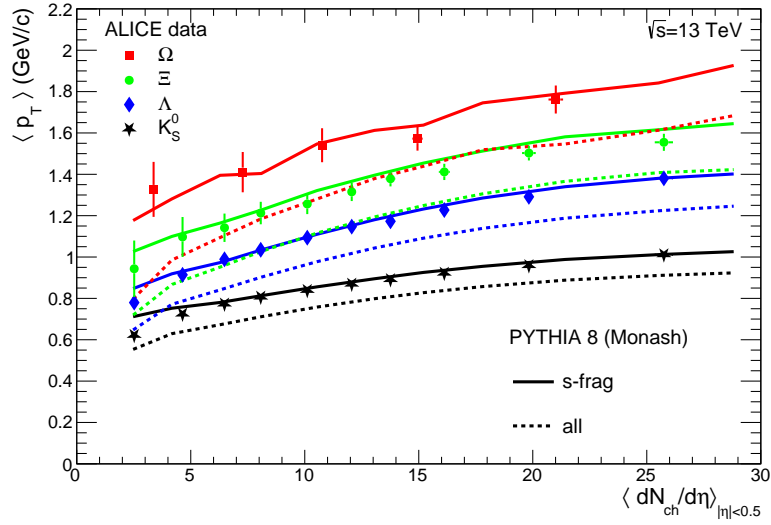


Figure 13: Measured average transverse momenta of strange particles (K_S^0 , Λ , Ξ , Ω) versus charged-particle multiplicity at midrapidity in pp collisions at $\sqrt{s} = 13$ TeV [5] compared with PYTHIA 8 (Monash) calculations. See Fig. 5 for the corresponding PYTHIA 6 (Perugia 2011) calculations.

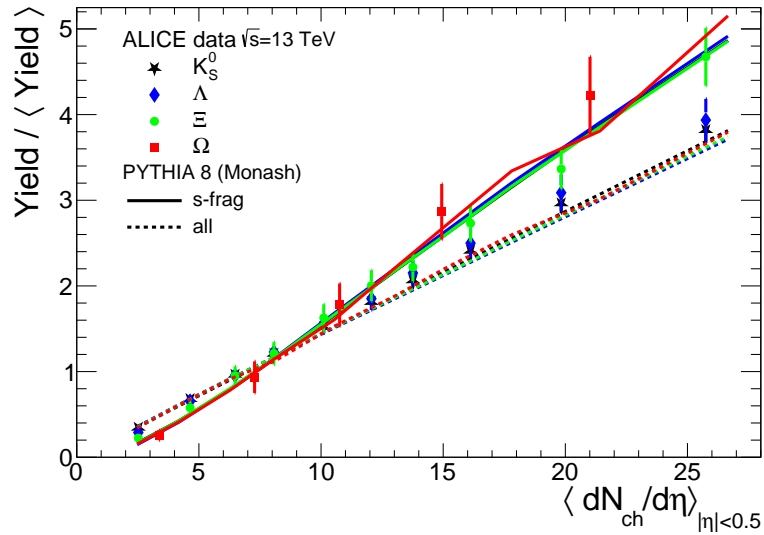


Figure 14: Self-normalized yields of strange particles (K_S^0 , Λ , Ξ , Ω) versus charged-particle multiplicity at midrapidity in pp collisions at $\sqrt{s} = 13$ TeV [5] compared with PYTHIA 8 (Monash) calculations. See Fig. 6 for the corresponding PYTHIA 6 (Perugia 2011) calculations.

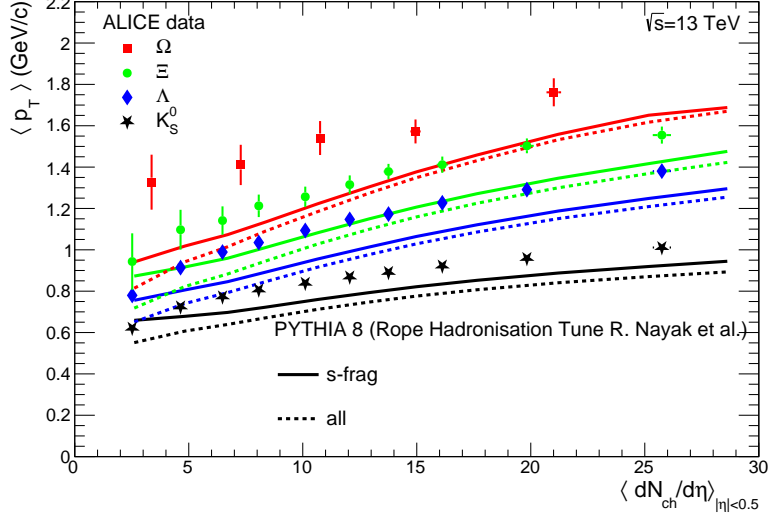


Figure 15: Measured average transverse momenta of strange particles (K_S^0 , Λ , Ξ , Ω) versus charged-particle multiplicity at midrapidity in pp collisions at $\sqrt{s} = 13$ TeV [5] compared with calculations of PYTHIA 8.306 with rope hadronization, with parameters by Nayak et al. as described in the text.

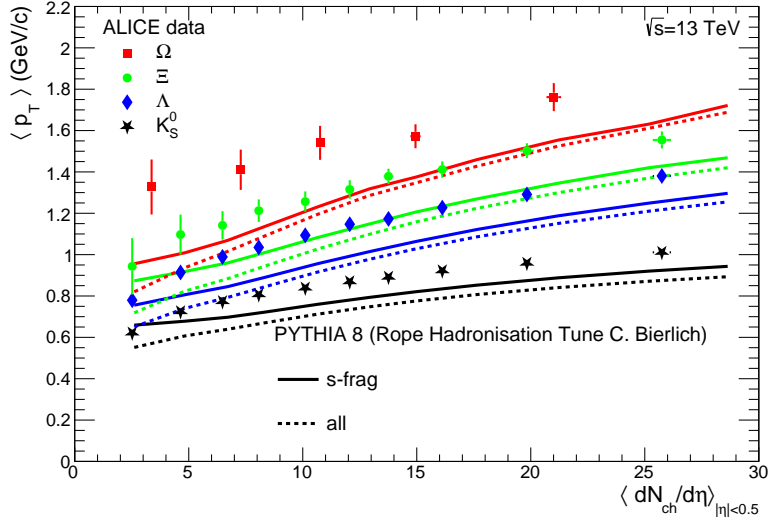


Figure 16: Same as Fig. 15 but with parameters from Bierlich.

B PYTHIA with rope hadronization

In Ref. [21] it is claimed that PYTHIA including the rope hadronization mechanism, which was introduced in [34], is able to describe yields and mean p_T of strange and multi-strange particles versus multiplicity in pp collisions at 7 and 13 TeV. We therefore repeated our calculations with the latest PYTHIA 8.306 and the following explicit settings for color reconnection and ropt hadronization:

```
// QCD based CR
pythia->ReadString("MultiPartonInteractions:pT0Ref = 2.15");
pythia->ReadString("BeamRemnants:remnantMode = 1");
pythia->ReadString("BeamRemnants:saturation = 5");
pythia->ReadString("ColourReconnection:mode = 1");
pythia->ReadString("ColourReconnection:allowDoubleJunRem = off");
pythia->ReadString("ColourReconnection:m0 = 0.3");
pythia->ReadString("ColourReconnection:allowJunctions = on");
pythia->ReadString("ColourReconnection:junctionCorrection = 1.2");
pythia->ReadString("ColourReconnection:timeDilationMode = 2");
pythia->ReadString("ColourReconnection:timeDilationPar = 0.18");
// Rope Hadronization
pythia->ReadString("Ropewalk:RopeHadronization = on");
pythia->ReadString("Ropewalk:doShoving = on");
pythia->ReadString("Ropewalk:doFlavour = on");
pythia->ReadString("Ropewalk:r0 = 0.5");
pythia->ReadString("Ropewalk:m0 = 0.2");
pythia->ReadString("Ropewalk:beta = 1.0");
// Set shoving strength to 0 explicitly
pythia->ReadString("Ropewalk:gAmplitude = 0.");
// Parton Vertex
pythia->ReadString("PartonVertex:setVertex = on");
pythia->ReadString("PartonVertex:protonRadius = 0.7");
pythia->ReadString("PartonVertex:emissionWidth = 0.1");
```

For the Nayak et al. parameters [21] we used

```
// Nayak et al. parameters
pythia->ReadString("Ropewalk:tInit = 1.0");
pythia->ReadString("Ropewalk:tShove = 10.");
pythia->ReadString("Ropewalk:deltat = 0.05");
```

For the Bierlich parameters (which he communicated to us by email) we used

```
// Bierlich parameters
pythia->ReadString("Ropewalk:beta = 0.1");
pythia->ReadString("Ropewalk:tInit = 1.5");
pythia->ReadString("Ropewalk:tShove = 0.1");
```

The respective results for the mean p_T versus multiplicity are shown in Fig. 15 for the Nayak et. al. and Fig. 16 for the Bierlich settings. To our surprise the results that are very similar for the two settings do not reveal the reported agreement with the data.